

**NASA  
Technical  
Memorandum**

**NASA TM-86512**

**DEVELOPMENT AND TEST OF ADVANCED  
COMPOSITE COMPONENTS**

**Center Director's Discretionary Fund Program**

**By Gwyn Faile, Rose Hollis, Frank Ledbetter,  
Juan Maldonado, Jim Sledd, Jim Stuckey,  
Gerald Waggoner, and Erich Engler**

**Structures and Propulsion Laboratory**

**June 1985**



**(NASA-TM-86512) DEVELOPMENT AND TEST OF  
ADVANCED COMPOSITE COMPONENTS. CENTER  
DIRECTOR'S DISCRETIONARY FUND PROGRAM (NASA)  
36 p HC A03/MF A01**

**CSCL 11D**

**N85-32147**

**Unclas  
21946**

**G3/24**



**National Aeronautics and  
Space Administration**

**George C. Marshall Space Flight Center**

1. REPORT NO. NASA TM-86512		2. GOVERNMENT ACCESSION NO.		3. RECIPIENT'S CATALOG NO.	
4. TITLE AND SUBTITLE Development and Test of Advanced Composite Components Center Director's Discretionary Fund Program				5. REPORT DATE June 1985	
				6. PERFORMING ORGANIZATION CODE	
7. AUTHOR(S) G. Falle, R. Hollis, F. Ledbetter, J. Maldonado, J. Sledd, J. Stuckey, G. Waggoner, and E. Engler				8. PERFORMING ORGANIZATION REPORT #	
9. PERFORMING ORGANIZATION NAME AND ADDRESS  George C. Marshall Space Flight Center Marshall Space Flight Center, Alabama 35812				10. WORK UNIT, NO.	
				11. CONTRACT OR GRANT NO.	
12. SPONSORING AGENCY NAME AND ADDRESS  National Aeronautics and Space Administration Washington, D.C. 20546				13. TYPE OF REPORT & PERIOD COVERED  Technical Memorandum	
				14. SPONSORING AGENCY CODE	
15. SUPPLEMENTARY NOTES  Prepared by Structures and Propulsion Laboratory, Science and Engineering.					
16. ABSTRACT  This report describes the design, analysis, fabrication, and test of a complex "bathtub fitting." Graphite fibers (P75) in an epoxy matrix were utilized in manufacturing of 11 components representing four different design and layup concepts. Design allowables were developed for use in the final stress analysis. Strain gage measurements were taken throughout the static load test and correlation of test and analysis data were performed, yielding good understanding of the material behavior and instrumentation requirements for future applications.					
17. KEY WORDS  Graphite Epoxy Composites Low CTE Components			18. DISTRIBUTION STATEMENT  Unclassified — Unlimited		
19. SECURITY CLASSIF. (of this report)  Unclassified		20. SECURITY CLASSIF. (of this page)  Unclassified		21. NO. OF PAGES  36	
				22. PRICE  NTIS	

## ACKNOWLEDGMENTS

A number of persons in various organizations had a significant role in the execution of this effort.

Personnel in the Structural Development Branch, Structures Engineering Branch, Polymers and Composites Branch, Structural Test Branch, Quality Control, and Developmental Sciences, Ontario, California, contributed to this task.

The authors offer their thanks to all contributors.

## TABLE OF CONTENTS

	Page
INTRODUCTION .....	1
COMPONENT DESIGN .....	3
MATERIAL CHARACTERIZATION .....	8
Equipment Used .....	8
Test Procedures .....	8
RESULTS AND DISCUSSION .....	9
Unidirectional Material .....	9
Quasi-Isotropic Material .....	9
STRUCTURAL ANALYSIS .....	11
COMPONENT FABRICATION .....	11
STRUCTURAL TEST .....	14
Summary .....	14
Test Description .....	14
Test Anomalies .....	14
Test Data .....	14
Test Results .....	14
CONCLUSIONS AND RECOMMENDATIONS .....	29

# LIST OF ILLUSTRATIONS

Figure	Title	Page
1.	Focal Plane Structure (FPS) .....	2
2.	Composite bathtub fitting.....	3
3.	Fitting No. 1 (27M10003) .....	4
4.	Fitting No. 2 (27M10001) .....	5
5.	Fitting No. 3 (27M10002) .....	6
6.	Fitting No. 4 (21M21009) .....	7
7.	Bathtub fitting finite element model.....	12
8.	Bathtub fitting in a composite structural test setup (view 1).....	16
9.	Bathtub fitting in a composite structural test setup (view 3).....	17
10.	Bathtub fitting mounting anomaly for Specimen 27M10003 SN1.....	18
11.	Strain gage and failure locations.....	20
12.	Strain gage and failure locations.....	23
13.	Strain gage and failure locations.....	26
14.	Strain gage locations .....	29
15.	Progressive failure analysis.....	30

# LIST OF TABLES

Table	Title	Page
1.	Properties of Unidirectional P75S/934 .....	10
2.	Properties of $(0/\pm 45/90)_{ns}$ P75S/934 .....	10
3.	Comparison of Elastic Properties for $(0/\pm 45/90)_{ns}$ P75S/934, Predicted Versus Measured .....	11
4.	Process and Cure Cycle Summary for DSI Part for NASA Drawing Number 27M10003-1 .....	13
5.	Test Results .....	15
6.	27M10001 S/N2 Strain Gage Test Data .....	19
7.	27M10001 Strain Gage Test Data .....	19
8.	27M10001 Strain Gage Test Data .....	20
9.	27M10002 Strain Gage Test Data .....	21
10.	27M10002 Strain Gage Test Data .....	21
11.	27M10002 Strain Gage Test Data .....	22
12.	27M10002 Comparison of Tests and SQ5 Results .....	22
13.	27M10002 Comparisor of Test and SQ5 Results .....	23
14.	27M10003 Strain Gage Test Data .....	24
15.	27M10003 Strain Gage Test Data .....	24
16.	27M10003 Strain Gage Test Data .....	25
17.	27M10003 Comparison of Test and SQ5 Results .....	25
18.	27M10003 Comparison of Test and SQ5 Results .....	26
19.	27M10009 Strain Gage Test Data .....	27
20.	27M10009 Strain Gage Test Data .....	27
21.	27M10009 Strain Gage Test Data .....	28
22.	27M10009 Comparison of Test and SQ5 Results .....	28
23.	27M10009 Comparison of Test and SQ5 Results .....	28

# TECHNICAL MEMORANDUM

## DEVELOPMENT AND TEST OF ADVANCED COMPOSITE COMPONENTS

### INTRODUCTION

The report documents the development effort to improve the design and load-carrying ability of a complex corner fitting, using advanced filament composites in a resin matrix (Epoxy).

The Optical Telescope Assembly portion of the Space Telescope contains a number of graphite epoxy structures. One of these structures is the Focal Plane Structure (FPS) (Fig. 1), a critical structural assembly requiring a high order of thermal stability, structural stiffness, and low weight. The graphite epoxy layup of the FPS is designed to achieve a coefficient of thermal expansion (CTE) of  $\pm 0.09 \times 10^{-6}$  in./in./°F. Among the components making up the FPS are eight brackets that provide support for the four radial instruments that are carried on the FPS. These eight brackets are of a configuration commonly known as "bathtub fittings" in aerospace structures parlance, and are of titanium.

The original design of these bathtub fittings, however, was of graphite epoxy with a pseudoisotropic layup to achieve the specified CTE. Structural testing of these bathtub fittings to 1.4 x limit load was required to verify the design. These fittings failed in test, some demonstrating an ultimate factor-of-safety of only 1.15 instead of the required 1.4 factor.

Due primarily to these unpredicted low factors (schedule was also an important deciding factor), the penalties in weight and pointing stability were accepted and the fittings were redesigned for titanium. As a number of new projects, such as AXAF, require optical benches with stringent dimensional stability during thermal excursion, application of graphite/epoxy composites will be required.

Existing technology is limited in design, analysis, fabrication, and test of complex components, fabricated from Pitch 75 graphite fibers, especially the effects of layup changes on the ultimate strength, the stress distribution and correlation of strain gage data to analysis results.

Since bathtub fittings are a common configuration for aerospace structures, it became obvious that development work for such fittings is required if graphite epoxy is to be a viable candidate for these structures.

The development objectives for this program were: evaluation of layup changes to improve ultimate strength of fabricated components, develop basic material data, establish analysis methods, and verify the design and analysis through test of full-size components.

In order to eliminate erroneous results, it was decided to fabricate and test three parts of each design. This would average the variations in as-fabricated properties and tolerances.

ORIGINAL PAGE IS  
OF POOR QUALITY

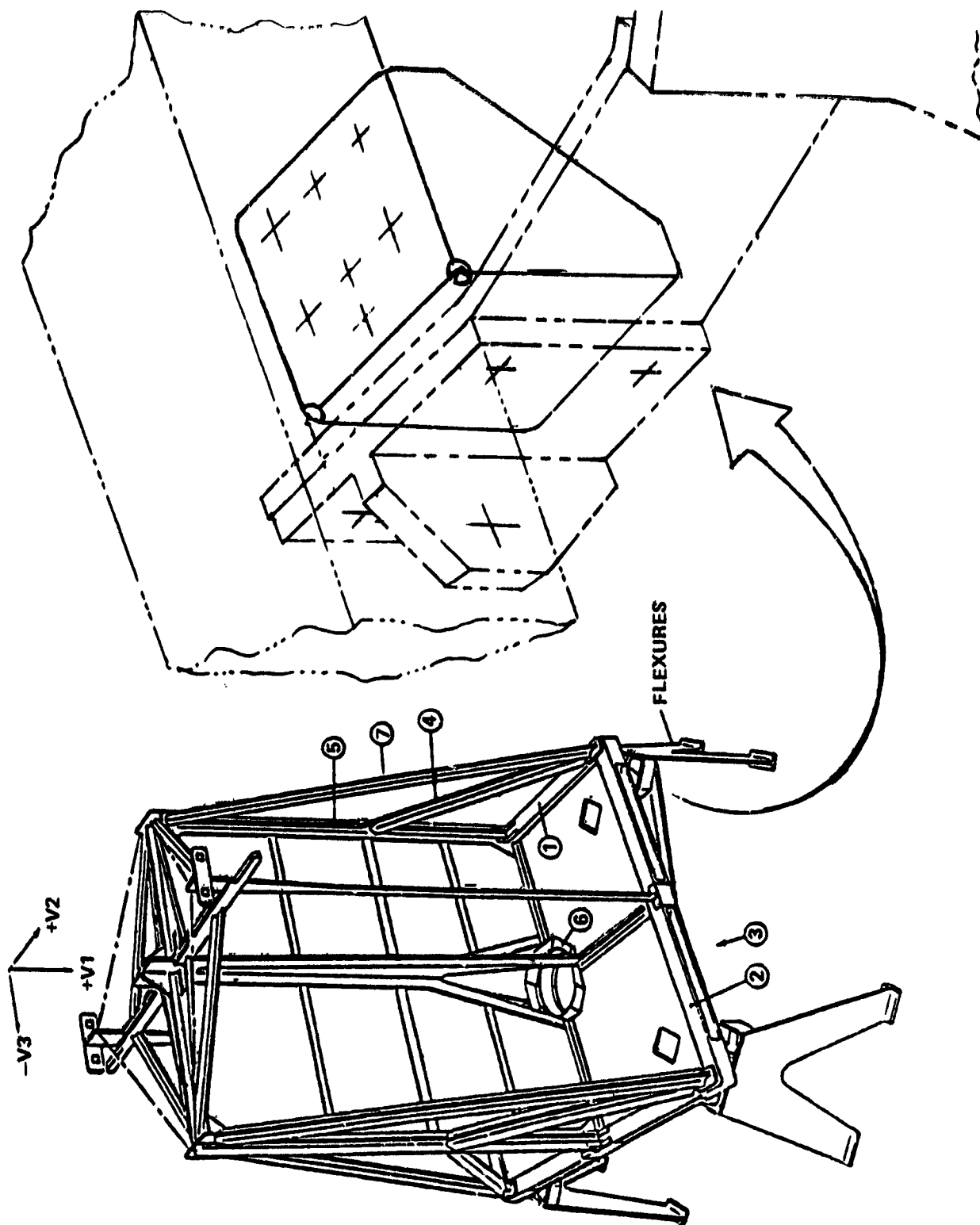


Figure 1. Focal Plane Structure (FPS).



## COMPONENT DESIGN

The component selected for the development effort has a complex shape, referred to as "bathtub fitting," and is shown in Figure 2. Four different designs were executed, differing from each other by the arrangement (layup) of the composite material. Designs are shown on Figures 3 through 6.

Analysis of the failed initial FPS bathtub fitting showed that the fractures developed along the laminate splice-lines. Due to the laminate flat pattern designs, these splice-lines lay along the corners of the fittings and had only a slight stagger between plies. The three layup patterns selected for this program were designed maintaining the same laminate material, fiber orientation, resin content, and basic dimensions of the P-E fittings. However, the layup patterns were modified to relocate the splice-lines in planes away from the corners. Also, radius fillers were added for the areas in contact with the test fixture and bolt heads.

The following discussion summarizes the design variations. Figure 2 details the basic dimensions, the radius fillers, and the alternating of the laminate flat patterns. Figure 3 shows the first design (27M1003) which is the original FPS bathtub fitting. Additional fittings of this design were fabricated to compare their fabrication quality to the originals — to minimize test errors due to variation in workmanship. Figure 4 gives another layup (27M1001) which relocated the splice-lines to the sides of the fitting with staggered splice-line angles of 30 deg and 60 deg. The third design, Figure 5 (27M10002), had overlapping "tabs" on the top and back planes so that each laminate had one continuous (not spliced) surface for each surface that was spliced. These additional tabs increased the wall thickness on these surfaces but afforded better continuity. The last design, Figure 6 (21M10009), is an assembly of three laminates, each of which provided continuity around the corners in one direction (a total of three laminates for the three viewing axis). Reduced drawings for all components are attached to the report.

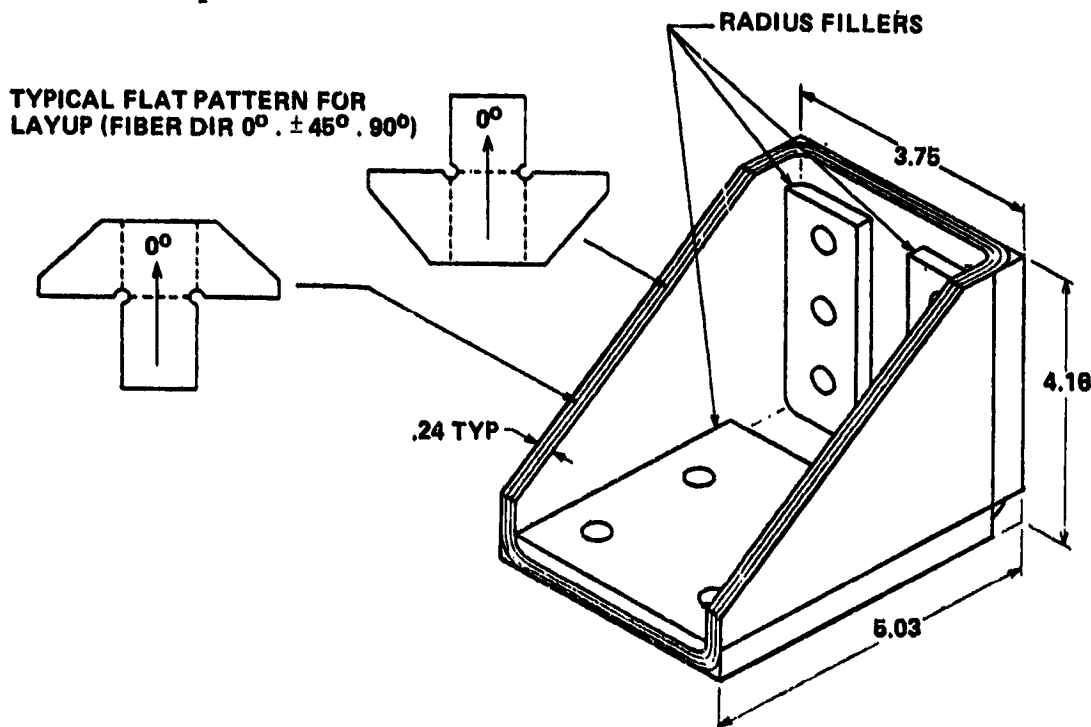
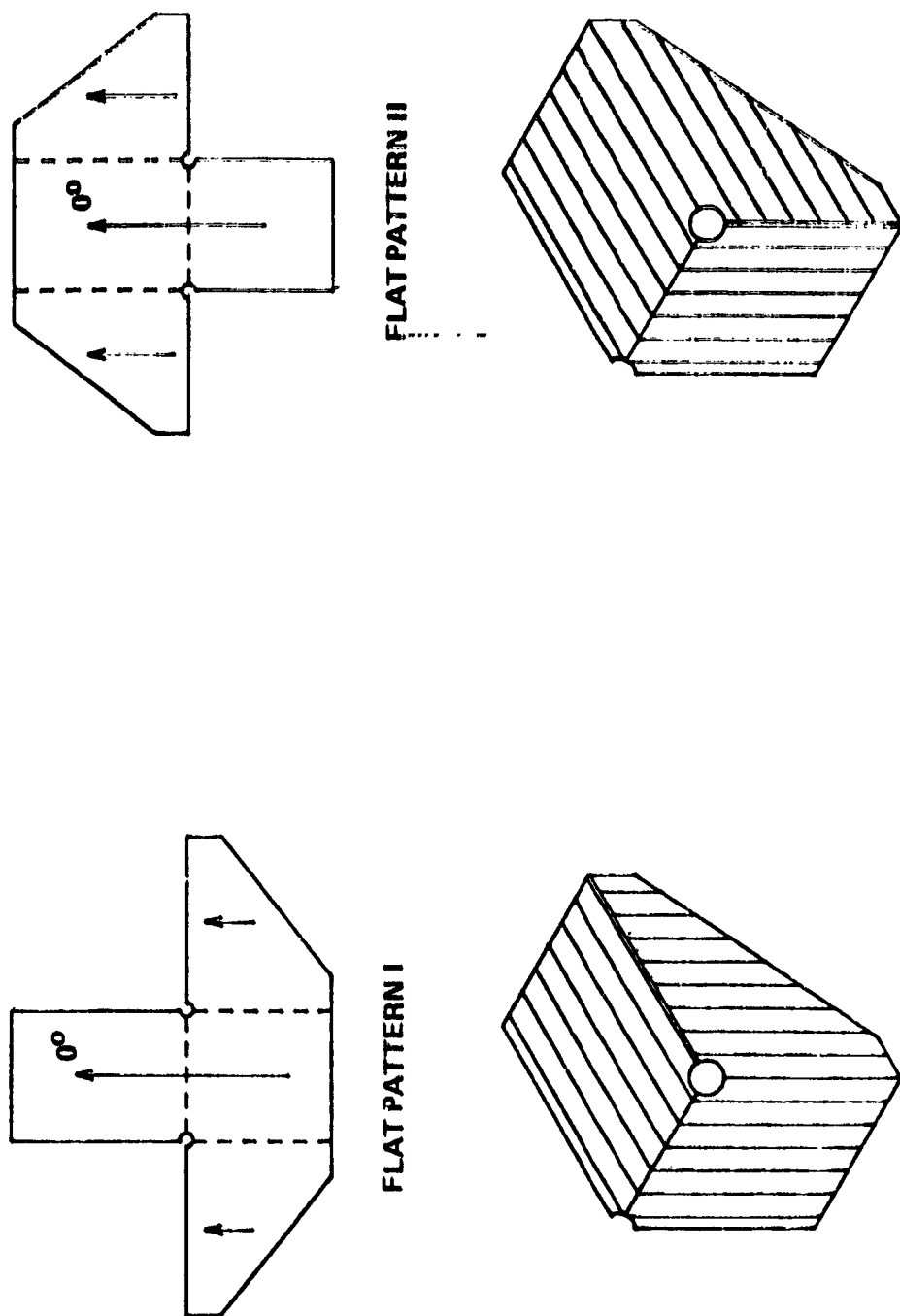
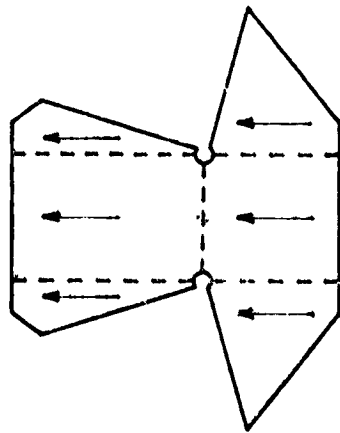


Figure 2. Composite bathtub fitting.

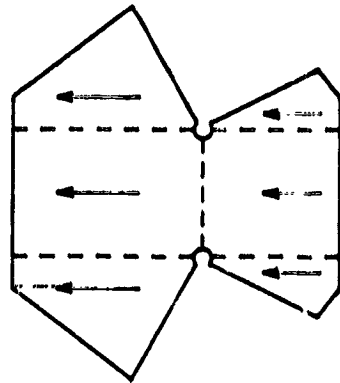


AS LAID-UP ON FITTING

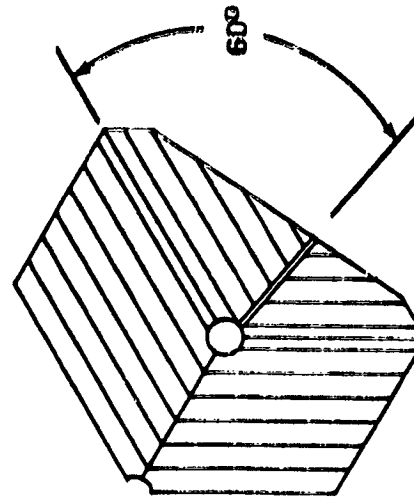
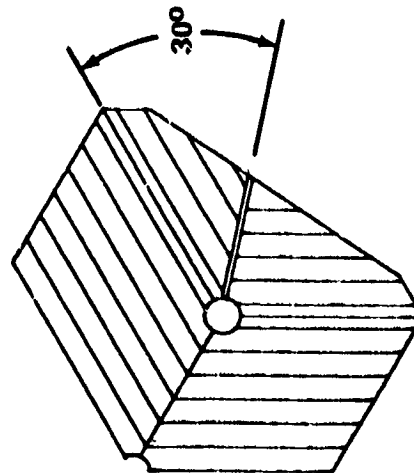
Figure 3. Fitting No. 1 (27M10003).



FLAT PATTERN I

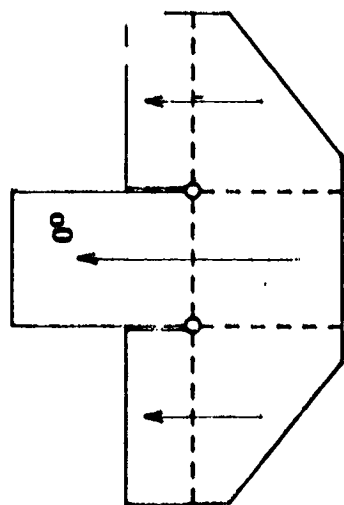


FLAT PATTERN II

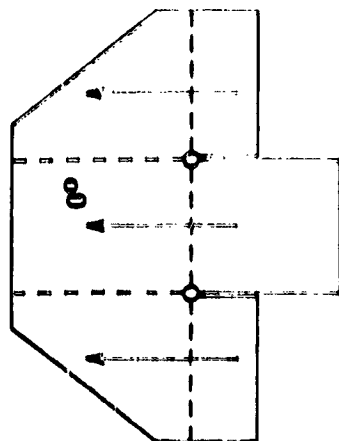
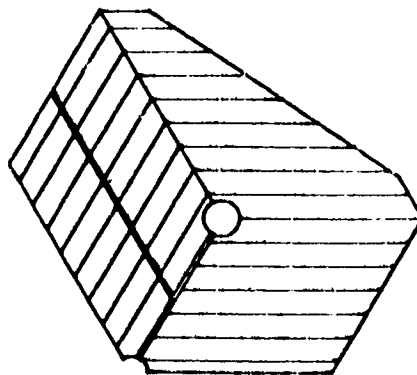


AS LAID-UP ON FITTING

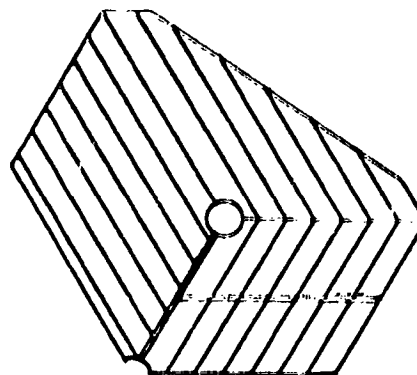
Figure 4. Fitting No. 2 (27M10001).



FLAT PATTERN I



FLAT PATTERN II



AS LAID-UP ON FITTING

Figure 5. Fitting No. 3 (27M100C2).

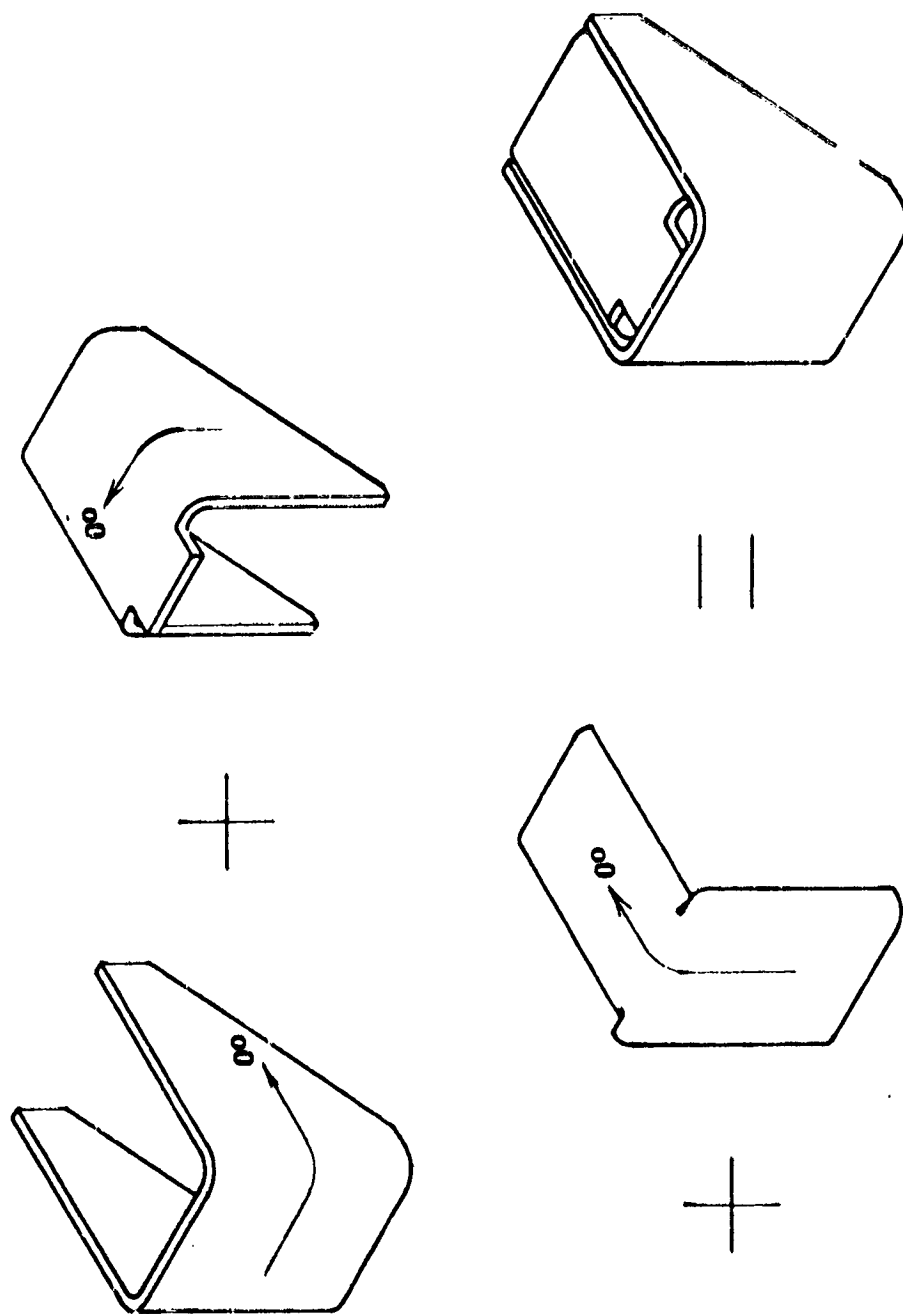


Figure 6. Fitting No. (31M21009).

## MATERIAL CHARACTERIZATION

The P75S/934 graphite/epoxy bathtub fittings were modeled using the finite element method in order to predict their behavior under actual loading conditions. For the model to be somewhat accurate, material properties of the system had to be determined. The material properties determined for this system include tensile, compressive, and shear properties for both unidirectional and quasi-isotropic (0/±45/90) laminates.

### Equipment Used

The P75S/934 tape was supplied by Fiberite, Inc., to Developmental Sciences, Inc., which then prepared laminates and supplied them to the Marshall Space Flight Center for characterization. The laminates were cut into the desired sample sizes by a water-cooled diamond saw, and holes were drilled in the laminates (when appropriate) by a water-cooled drill press. An Instron 1125 mechanical testing machine, in conjunction with a Fluke 2450 MCS data acquisition system, was used to determine the mechanical properties of the material. Fiber volume fractions were obtained by determining the density of the composite material and then, assuming no voids were present, comparing that density with the reported densities for the fiber and resin as supplied by Fiberite to determine the fiber volume fraction.

### Test Procedures

#### Unidirectional Material

Tensile tests were performed on unidirectional material to determine longitudinal and transverse Young's Moduli,  $E_1$  and  $E_2$ , longitudinal and transverse ultimate strengths,  $F_0^{tu}$  and  $F_{90}^{tu}$ , and the major Poisson's ratio  $\nu_{12}$ . The tests were performed according to ASTM D3039-76. 8-ply laminates with specimen dimensions 0.500 in. wide by 9.00 in. long, using a 6.00-in. gage length, were used to determine  $E_1$ ,  $F_0^{tu}$ , and  $\nu_{12}$ ; 16-ply laminates, with specimen dimensions 1.000 in. wide by 6.50 in. long, using a 3.50-in. gage length, were used to determine  $E_2$  and  $F_{90}^{tu}$ .

Compression tests were performed to determine  $F_0^{cu}$  and  $F_{90}^{cu}$ , the longitudinal and transverse compressive strengths, respectively. The test method used was ASTM D3410-75 (the Cleanese test fixture). 16-ply laminates, with specimen dimensions 0.250 in. wide by 5.5 in. long, using a 0.500-in. gage length, were used to determine both  $F_0^{cu}$  and  $F_{90}^{cu}$ .

In-plane shear tests were performed to determine the inplane shear modulus  $G_{12}$  in the inplane shear strength  $F^{su}$ . Two different tests were used to determine these properties.  $G_{12}$  was determined by the three-rail shear test (in ASTM, committee, not published), and  $F^{su}$  was determined by the 45 deg off-axis tensile test (same procedure as ASTM D3039-76). 16-ply laminates were used for both procedures; sample

dimensions were 6.00 in. by 6.00 in. with nine approximately spaced 0.5-in. diameter holes for the rail shear test and 1.00 in. wide by 9.00 in. long with a 6.00-in. gage length for the 45 deg off-axis test.

### Quasi-Isotropic Material

Tensile tests on quasi-isotropic material were performed to determine  $E_x$ ,  $F_x^{tu}$ , and  $\nu_{xy}$ , the longitudinal (and transverse) Young's Modulus, ultimate tensile strength, and Poisson's ratio, respectively. 16-ply laminates ( $0/\pm 45/90_{2s}$ ) and 24-ply laminates ( $0/\pm 45/90_{3s}$ ) were both used for comparative purposes. Sample dimensions were identical to those for the 90 deg tensile tests.

Compression tests were used to determine  $F_c^{cu}$ , the longitudinal (and transverse) compressive strength. 16-ply laminates were used, and sample dimensions were identical to those used on unidirectional material.

Three-rail shear tests were used to determine the inplane shear modulus and shear strength,  $G_{xy}$  and  $F^{su}$ . Both 16-ply and 24-ply laminates were used, and specimen dimensions were identical to those for the unidirectional material.

## RESULTS AND DISCUSSION

The material properties that were determined agree well with those obtained in other laboratories for the same material. All properties may be found in Tables 1 and 2, including fiber volume fractions.

### Unidirectional Material

Based on the fiber volume fraction and the given properties for the P75S fibers, the results for the unidirectional material seem reasonable, allowing for discrepancies in the determination of the fiber volume fraction.

One problem that did occur in the characterization of the unidirectional material was obtaining a representative inplane shear strength. The rail shear test results in very low shear strengths for unidirectional material, so the 45 deg off-axis tensile test was used to determine shear strength. However, the strengths that are obtained by this method can be as much as 30 to 40 percent low. Thus, the values obtained may be very conservative.

### Quasi-Isotropic Material

Elastic properties ( $E_x$ ,  $\nu_{xy}$ ,  $G_{xy}$ ) for quasi-isotropic material can be predicted, based on unidirectional properties, by the use of classical lamination theory (CLT). The properties that were measured could be compared with those that were predicted.

The Young's Modulus obtained for 16-ply laminates agreed well with that predicted by CLT; however, the Poisson's ratio and inplane shear modulus did not. The Poisson's ratio was not good, probably because of poor strain gages, and the shear modulus was not good because of testing problems. Because of a lack of any more 16-ply material, 24-ply materials were tested to obtain better results.

TABLE 1. PROPERTIES OF UNIDIRECTIONAL P75S/934

		$V_f$
$E_1$ , Msi	39.2	0.56
$E_2$ , Msi	1.14	0.60
$G_{12}$ , Msi	0.574	0.60
$\nu_{12}$ , Msi	0.337	0.56
$F_0^{tu}$ , ksi	105.5	---
$F_0^{cu}$ , ksi	42.0	---
$F_{90}^{tu}$ , ksi	3.03	---
$F_{90}^{cu}$ , ksi	15.8	---
$F^{su}$ , ksi	3.02	---

TABLE 2. PROPERTIES OF  $(0/\pm 45/90)_{ns}$  P75S/934

		No. of Plies	$V_f$
$E_x$ , Msi	14.6	16	0.57
$G_{xy}$ , Msi	5.16	24	0.58
$\nu_{xy}$	0.343	24	0.58
$F_x^{tu}$ , ksi	39.4	16	---
$F_x^{cu}$ , ksi	28.0	16	---
$F^{cu}$ , ksi	5.62	16	---

The Poisson's ratio and inplane shear modulus agreed with theory for the 24-ply material, but the Young's modulus did not. One inference that may be made is that the Young's modulus may be thickness-dependent, while the other two elastic properties may or may not be dependent on thickness. Table 3 compares CLT values with the actual measured values for the material.

Although strength properties cannot be predicted by CLT, the results were within reason for a quasi-isotropic laminate, compared to the unidirectional properties.



The inplane shear strength may again be too conservative, and is based on the 16-ply tests because the loads required on the 24-ply samples were so great that the samples slipped in the test fixture. --

TABLE 3. COMPARISON OF ELASTIC PROPERTIES FOR (0/±45/90)<sub>ns</sub>  
P75S/934, PREDICTED VERSUS MEASURED

	<u>Predicted</u>	<u>Measured</u>	
		<u>16 Plies</u>	<u>24 Plies</u>
$E_x$ , Msi	13.9	14.6	11.4
$G_{xy}$ , Msi	5.25	4.30 <sup>a</sup>	5.16
$\nu_{xy}$	0.325	0.376 <sup>b</sup>	0.343

a. Slippage in fixture and possible strain gage bonding problems.

b. Possible strain gage bonding problems.

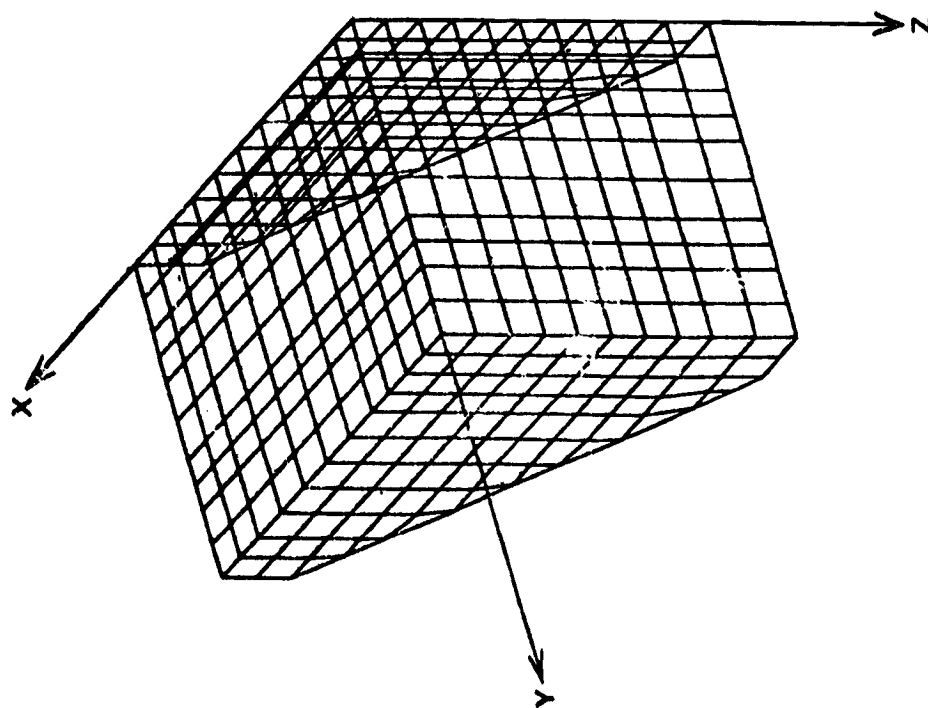
### STRUCTURAL ANALYSIS

The finite element method and classical lamination theory were used to perform the analysis. A finite element program (SPAR) was used in an uncoupled format to calculate laminate in-plane force resultants ( $N_x$ ,  $N_y$ ,  $N_{xy}$ ) and moment resultants ( $M_x$ ,  $M_y$ ,  $M_{xy}$ ). These were then input into a laminate point stress analysis program (SQ5) to calculate surface strains, which were compared with test strain gage data. The finite element model is present in Figure 7.

### COMPONENT FABRICATION

The composite components were fabricated under contract by Development Sciences, Inc., 15757 E. Valley Boulevard, P.O. Box 1264, City of Industry, California 91749. Also included were the production of the flat panels needed for material characterization samples. The individual layers were cut according to the template pattern and laid up on a male steel mold with approximately 1 in. excess for trimming to final dimensions. A precompaction operation was performed after every eight plies to eliminate voids and wrinkles (Table 4). The prepreg used was P75/934, supplied by Fiberite Corporation, and the parts were processed as shown on Table 4, including the bonding operation required for parts 21M1009. The ply orientations were inspected during layup and before bagging of the completed part. After curing, the holes were drilled and final contour machined. Similar inspection was required for the flat panels. Shipping inspection at the contractor plant, including dimensional verification or deviation documentation, was performed. At MSFC, the parts were inspected for dimensional conformance and overall appearance.

UNDEFORMED PRIOR TO LOADING



DEFORMED AFTER LOADING

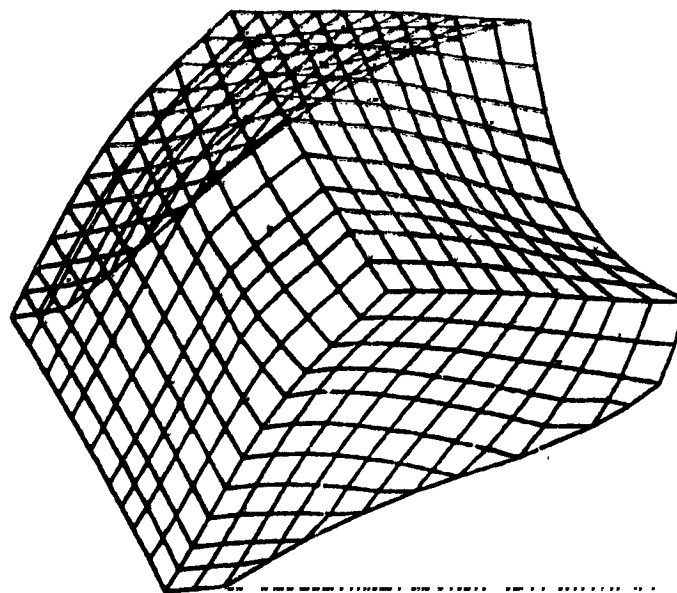


Figure 7. Bathtub fitting finite element model.

TABLE 4. PROCESS AND CURE CYCLE SUMMARY FOR  
DSI PART FOR NASA DRAWING NUMBER 27M10003-1

1. Pre-compaction - every 8 plies @ 150°F and 7 psi (vacuum only) 1.0 hr.
2. Cure
  1. Place in A/C draw full vacuum ( $26 \pm 2$ " Hg)
  2. Pressurize to  $100 \pm 5$  psig - vent vacuum to atmosphere @ 25 psig
  3. Ramp Heat-up @  $2-5^\circ\text{F}/\text{min}$  to  $250^\circ\text{F} \pm 10^\circ\text{F}$
  4. Hold  $250^\circ\text{F}$  60 min.
  5. Ramp Heat-up @  $2-5^\circ\text{F}/\text{min}$  to  $350^\circ\text{F} \pm 10^\circ\text{F}$
  6. Hold  $350^\circ\text{F}$  120 min.
  7. Cool down under pressure @  $2 \pm 1^\circ\text{F}/\text{min}$  to  $150^\circ\text{F}$  max.
  8. Release pressure and remove from A/C.
3. Bond and Post Cure
  1. Apply \*EA934 to all faying surfaces - apply mechanical pressure to  $\approx 20$  psi
  2. Place in air convected oven
  3. Heat-up @  $2-5^\circ\text{F}/\text{min}$  to  $150^\circ\text{F} \pm 10^\circ\text{F}$
  4. Hold 30 min @  $150^\circ\text{F}$
  5. Heat-up @  $2-5^\circ/\text{min}$  to  $250^\circ\text{F} \pm 10^\circ\text{F}$
  6. Hold 30 min @  $250^\circ\text{F}$
  7. Heat-up @  $2-5^\circ\text{F}/\text{min}$  to  $350^\circ\text{F} \pm 10^\circ\text{F}$
  8. Hold 480 min (8 hrs) @  $350^\circ\text{F}$
  9. Cool Down @  $2^\circ \pm 1^\circ\text{F}$  to  $150^\circ\text{F}$
  10. Remove from oven.

Cure charts available for pre-compaction and cure.

\*EA934 is an asbestos filled adhesive per the included data sheets 1 through 3.

### Results

Inspection of delivered parts at MSFC revealed the following: all thicknesses, which are determined by the number of plies, were approximately 20 percent above the the specified dimensions on the drawings. The discrepancy was traced to the fact that the contractor had ordered a prepreg material with a Fiber Area Weight (FAW) of  $159 \text{ gr}/\text{m}^2$  with a resin content of 37 percent by weight. In order to achieve a nominal cured layer thickness of 0.005 in., the required FAW would be  $142 \text{ g}/\text{m}^2$ . As the contractor had used the material with the higher FAW and complied with the prescribed resin content (37 percent by weight), the ply thickness increased to 0.0062 and all dimensions depending on the number of layers increased accordingly. This change was accounted for in the analysis and material property documentation. Furthermore, due to the layup on a male mandrel, the interfaces to the test fixtures were not always flat and some shimming was required.

## STRUCTURAL TEST

### Summary

The composite material "bathtub" fittings were loaded to failure during the period of November 7, 1984, to July 10, 1984. The ultimate failure load varied from a low of 2,229 lb to a high of 4,492 lb. Table 5 gives a listing of the test specimen and the ultimate failure load.

### Test Description

Each "bathtub" fitting was instrumented with strain gages as per requirements of the stress analyst. The component was then installed into the test setup (Fig. 8 and 9) with mechanical measurements to verify the alignment. Two deflection gages were utilized, one to monitor movement/deflection of the support structure and one to monitor the deflection of the "bathtub" fitting.

The loading sequence for the first test specimen was as follows: (a) compressive load of 1,000 lb and return to zero; and (b) tension load until failure. All succeeding specimen were loaded to 1,000 lb tension (increments of 250 lb) then returned to zero. The procedure was repeated until an acceptable repeat of zero was obtained. A tension load was then applied until the test specimen failed. The load, deflection, and strains were recorded, beginning prior to start of loading and ending after test specimen failure, at a rate of 1 scan per 200 msec.

### Test Anomalies

The test specimen, 27M10003 SN-1 did not have fillet inserts. When the specimen was installed into the test fixture, there were gaps between the specimen and the test fixture. The procedure used for attaching the specimen was as follows: the two lower bolts were torqued first, then the two top bolts. After torquing, the gaps between the specimen and the mounting surface were measured. Figure 10 illustrates the condition that existed.

The deflection gages were inoperative during the testing of specimens 6, 7, 8, and 9. This was the result of an equipment malfunction that was not detected until test preparation for specimen 10.

### Test Data

A printout of all test data was furnished at the completion of the test for each specimen. The data tapes will be retained for a period of one year.

### Test Results

Table 5 presents the ultimate failure loads. The results for each group of fittings are presented in the following four sections.

TABLE 5. TEST RESULTS

<u>Bathtub Fitting</u>	<u>Date Tested</u>	<u>Ultimate Failure Load (lbs)</u>
27M10001 S/N3	11-4-83	4046
27M10001 S/N4	2-14-84	3703
27M10001 S/N2	5-17-84	3492
27M10002 S/N2	6-20-84	4492
27M10002 S/N4	6-21-84	4083
27M10002 S/N3	7-9-84	4387
27M10003 S/N1	7-9-84	2229*
27M10003 S/N2	7-9-84	3266
27M10003 S/N3	7-9-84	3659
27M10009 S/N2	7-10-84	3237
27M10009 S/N1	7-10-84	3015

\* Did not have radius insert.

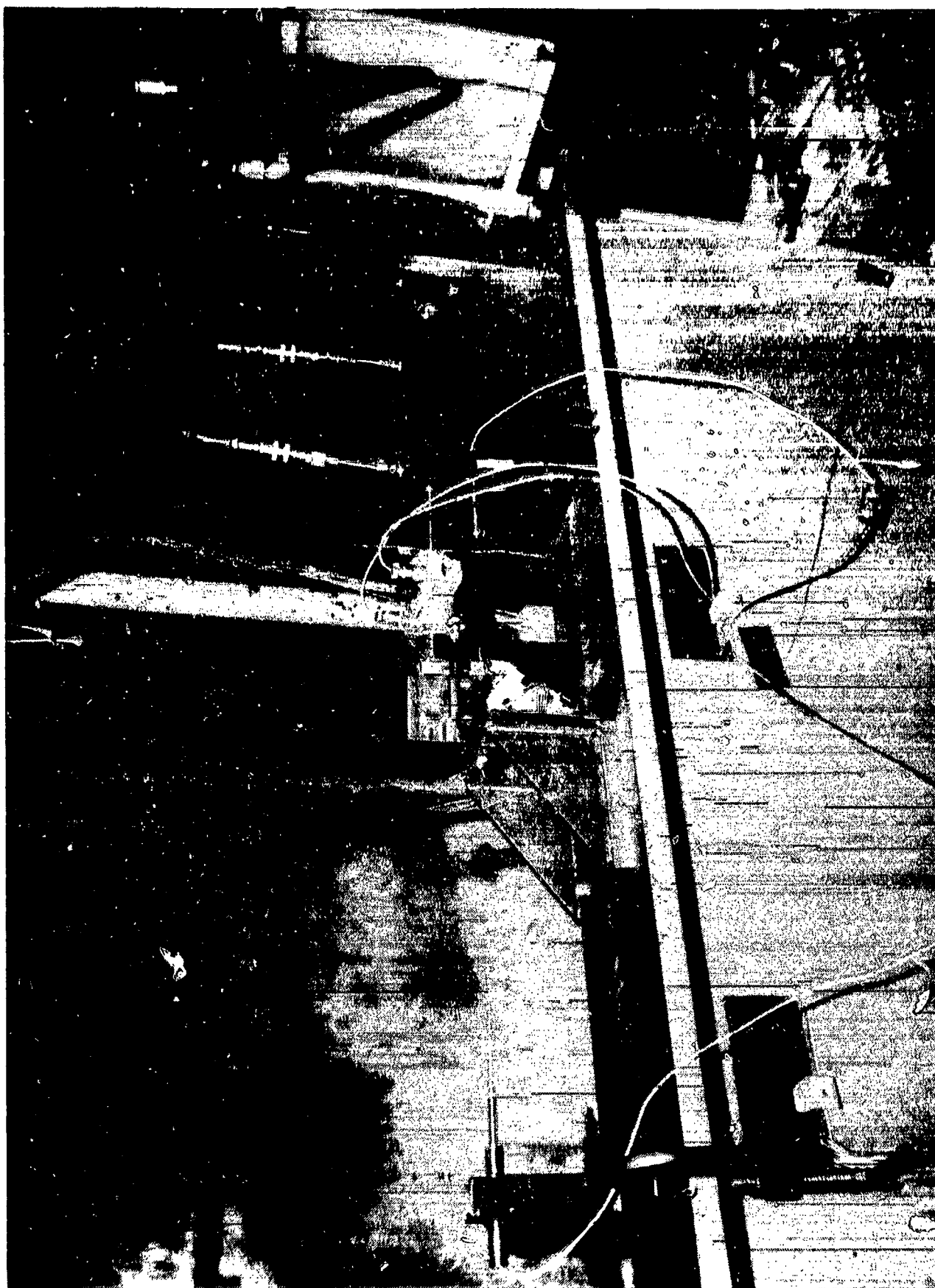


Figure 8. Bathtub fitting in a composite structural test setup (view 1).

ORIGINAL DOCUMENT  
OF POOR QUALITY



Figure 9. Bathtub fitting in a composite structural test setup (view 3).

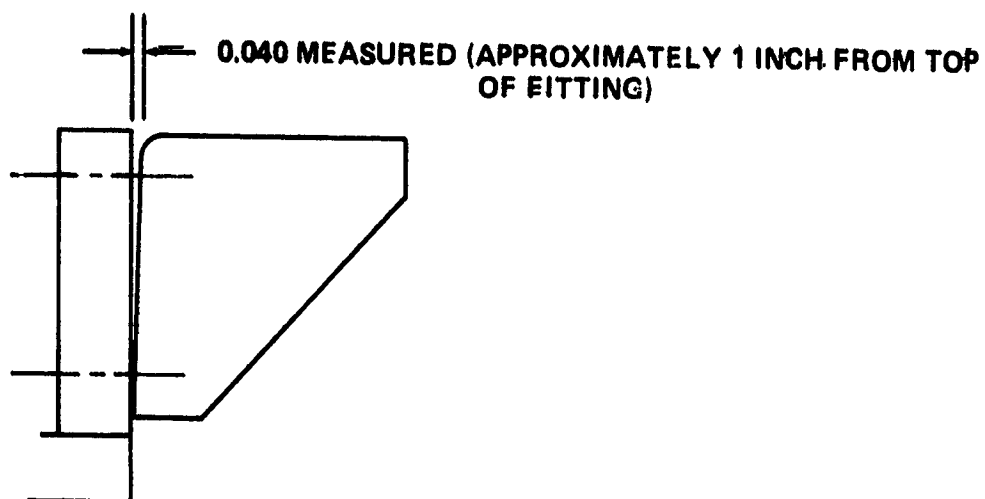
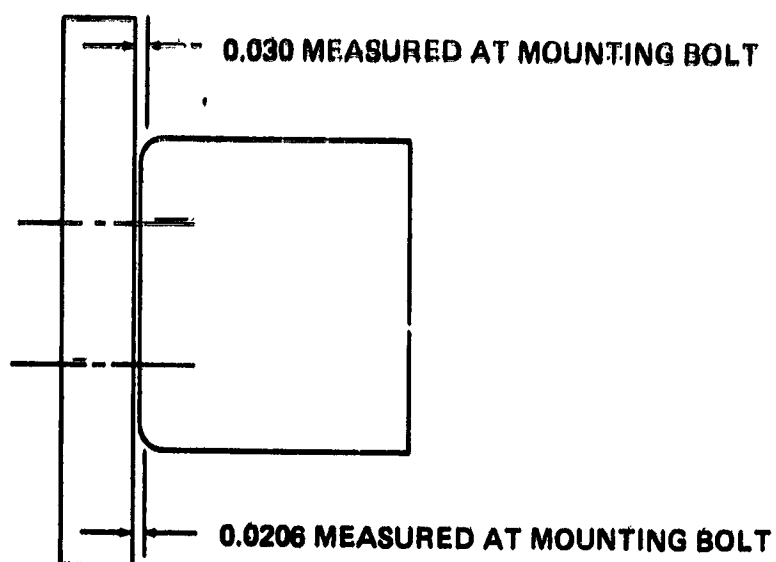


Figure 10. Bathtub fitting mounting anomaly for Specimen 27M10003 SN1.



# 1. 27M10001 Test Results

There was a problem with the kapton backing used for the first test, S/N 3, and 66 percent of the 82 channels did not provide data suitable for evaluation purposes. Kapton was not used on any of the following tests, and the number of channels was reduced to 39 for S/N2 and S/N4. Channels 1T13 and 3T13 were lost on S/N2, and channel 1T13 was lost on S/N4. Also, other strain gage locations were not optimal. They were located either too close to free edges or too close to the seams of the laminate layup. Data for three of these locations are presented in Tables 6 through 8. Location of these strain gages is presented on Figure 11. On the remaining fittings, it was decided to reduce the number of channels to 9 (3 rosettes) and to place the strain gages in locations where failures occurred.

TABLE 6. 27M10001 S/N2 STRAIN GAGE TEST DATA ( $\mu\text{in./in.}$ )

<u>Load (lb)</u>	<u>3T1</u>	<u>3T2</u>	<u>3T3</u>	<u>12T1</u>	<u>12T2</u>	<u>12T3</u>
0	6	3	3	3	3	6
276	24	43	-3	33	-12	12
505	43	66	6	55	-24	21
1105	85	143	-12	118	-58	48
1536	106	203	-12	161	-82	73
1960	137	270	-12	197	-106	100
2492	155	385	-3	221	-130	139
2994	161	498	-21	215	-143	160

These are strain gages in the same location on opposite sites of the fitting. (Refer to Figure 11.)

TABLE 7. 27M10001 STRAIN GAGE TEST DATA ( $\mu\text{in./in.}$ )

	<u>S/N4</u>			<u>S/N2</u>			<u>S/N4</u>			<u>S/N2</u>		
<u>Loads (lb)</u>	<u>7T1</u>	<u>7T2</u>	<u>7T3</u>	<u>7T1</u>	<u>7T2</u>	<u>7T3</u>	<u>8T1</u>	<u>8T2</u>	<u>8T3</u>	<u>8T1</u>	<u>8T2</u>	<u>8T3</u>
0	-6	-3	-3	3	3	3	-3	0	-3	3	3	3
242	3	-3	3	-6	6	-12	19	-3	-80	52	-3	-6
529	10	-3	13	-23	6	-30	51	-3	-170	103	-12	-18
1045	26	-3	26	-49	9	-61	99	-6	-330	203	-31	-42
1505	45	-6	42	-103	18	-94	151	-6	-487	334	-67	-79
2010	67	-10	54	-155	33	-128	212	-10	-673	455	-116	-115
2519	90	-16	71	-325	103	-94	276	-6	-868	713	-186	-191
3031	128	-19	90	-547	131	-97	386	0	-1140	989	-204	-240

These are strain gages in the same location on two different fittings with the same design. (Refer to Figure 11.)

TABLE 8. 27M10001 STRAIN GAGE TEST DATA ( $\mu\text{in./in.}$ )

Loads (lb)	S/N4			S/N2			S/N4			S/N2		
	9T1	9T2	9T3	9T1	9T2	9T3	10T1	10T2	10T3	10T1	10T2	10T3
0	-3	-3	-10	3	0	3	-3	-3	-3	3	0	3
242	48	20	-10	21	24	12	-10	-20	-20	-40	-37	3
520	110	64	-10	46	48	24	-20	-60	-61	-103	-70	0
1045	210	136	-23	85	91	42	-48	-103	-119	-209	-152	0
1505	319	200	-23	124	133	61	-64	-158	-190	-297	-238	3
2010	422	271	-23	176	181	76	-77	-213	-267	-384	-326	-9
2519	510	338	-13	155	209	112	-77	-261	-354	-340	-342	-64
3031	522	383	42	36	148	118	-90	-325	-425	-161	-299	-112

These are strain gages in the same location on two different fittings with the same design. (Refer to Figure 11.)

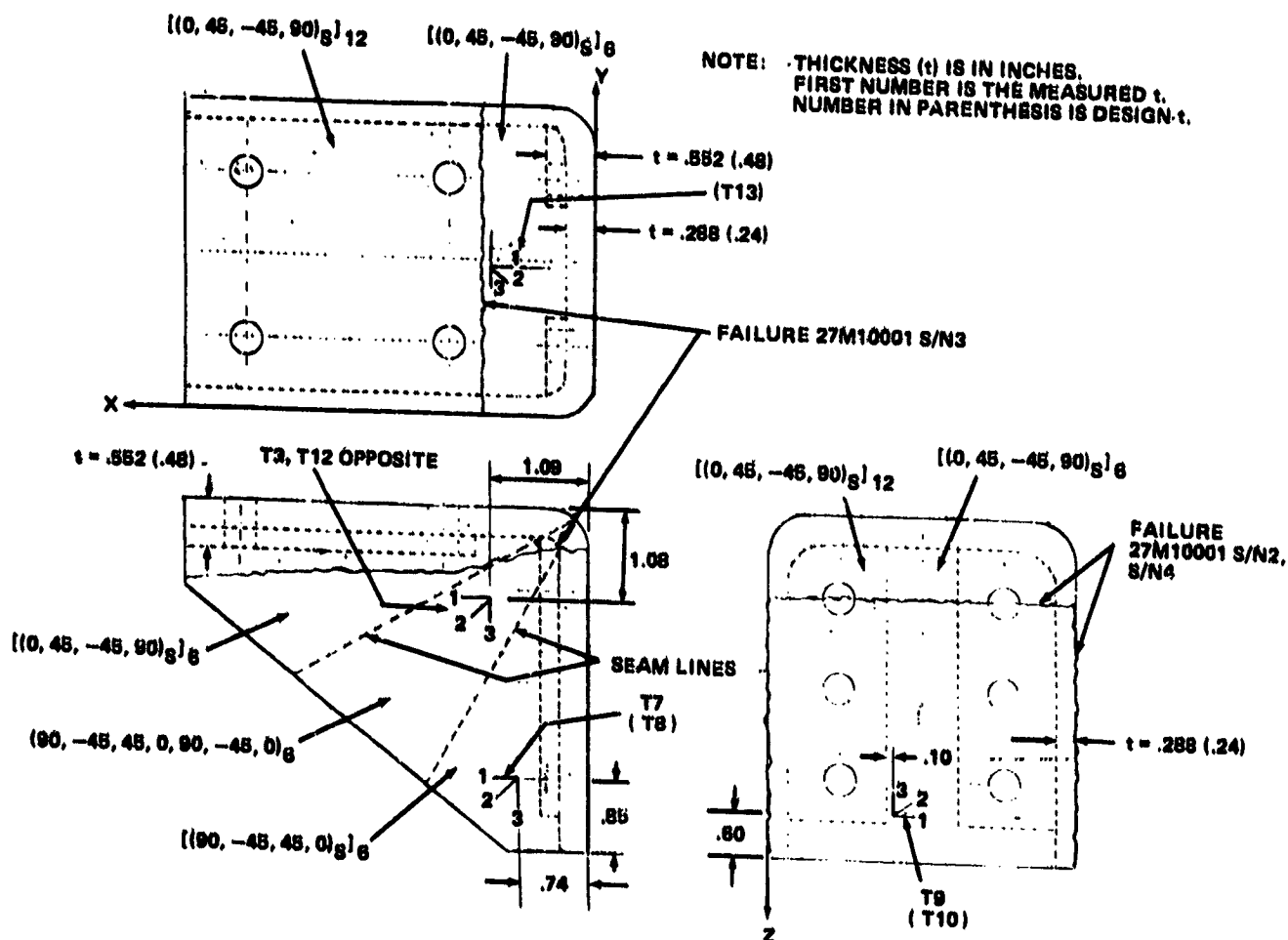


Figure 11. Strain gage and failure locations.

## 2. 2710002 Test Results

Tables 9 through 11 present strain gage test data. Tables 12 and 13 present comparison of test and analytical results. Locations of strain gages are presented on Figure 12. The three fittings failed across the bolt holes on the x-face at an average load of 4321 lb. This was the highest average failure load of all four test configurations.

TABLE 9. 27M10002 STRAIN GAGE TEST DATA ( $\mu\text{in./in.}$ )

Load (lb)	1T13			2T13			3T13		
	S/N2	S/N3	S/N4	S/N2	S/N3	S/N4	S/N2	S/N3	S/N4
500	134	143	149	58	39	01	0	-21	0
1000	288	310	313	136	88	194	6	-43	18
1500	479	495	480	242	166	294	27	-58	0
2000	686	699	647	364	254	391	55	-67	-18
2500	895	924	829	488	364	497	88	-73	-39
3000	1104	1148	1006	627	479	585	134	-73	-61
3500	1320	1404	1173	772	615	651	182	-73	-88
4000	1517	1750	1364	933	812	663	237	-61	-167
4300	1626	1987		1015	906		270	-67	
4400	1690			1066			270		

TABLE 10. 27M10002 STRAIN GAGE TEST DATA ( $\mu\text{in./in.}$ )

Load (lb)	1T14			2T14			3T14		
	S/N2	S/N3	S/N4	S/N2	S/N3	S/N4	S/N2	S/N3	S/N4
500	58	43	61	6	-24	-3	-67	-101	-91
1000	115	82	125	12	-52	-9	-140	-213	-185
1500	173	122	185	12	-82	-18	-225	-323	-282
2000	237	164	252	0	-115	-36	-328	-436	-394
2500	325	207	337	-3	-149	-58	-449	-554	-525
3000	437	249	443	-27	-185	-79	-595	-676	-683
3500	562	304	580	-45	-218	-109	-758	-816	-880
4000	735	386	1069	-85	-264	-400	-998	-993	-1793
4300	947	465		-172	-303		-1317	-1145	
4400	1193			-305			-1717		

TABLE 11. 27M10002 STRAIN GAGE TEST DATA ( $\mu\text{in./in.}$ )

<u>Loads (lb)</u>	1T15			2T15			3T15		
	<u>S/N2</u>	<u>S/N3</u>	<u>S/N4</u>	<u>S/N2</u>	<u>S/N3</u>	<u>S/N4</u>	<u>S/N2</u>	<u>S/N3</u>	<u>S/N4</u>
500	-40	-36	-46	0	-6	-9	39	52	46
1000	-79	-73	-88	-9	-15	-18	85	100	97
1500	-118	-109	-131	-12	-24	-24	136	149	152
2000	-161	-143	-176	-18	-30	-27	191	197	212
2500	-207	-182	-222	-27	-36	-24	249	249	273
3000	-270	-219	-282	-33	-43	-27	321	297	358
3500	-343	-255	-361	-40	-58	-33	403	355	461
4000	-452	-306	-723	-36	-82	155	522	421	958
4300	-601	-364		-9	-112		679	485	
4400	-726			46			840		

TABLE 12. 27M10002 COMPARISON OF TESTS AND SQ5 RESULTS ( $\mu\text{in./in.}$ )

Analysis at 2500 lb (before audible fiber breakage):

	<u>SQ5</u> <u>T13</u>	<u>S/N2</u> <u>T13</u>	<u>S/N3</u> <u>T13</u>	<u>S/N4</u> <u>T13</u>
$\epsilon_x$	-895 <sup>b</sup>	895	924	829
$\epsilon_y$	-141	88	-73	-39
$\gamma_{xy}$ <sup>a</sup>	$\pm 32$	$\pm 7$	$\pm 123$	$\pm 204$

a. Strain gages were not oriented consistently.

b. Probable test polarity problem. This surface is in compression.

TABLE 13. 27M10002 COMPARISON OF TEST AND SQ5 RESULTS ( $\mu\text{in./in.}$ )

	SQ5		S/N2		S/N3		S/N4	
	<u>T14</u>	<u>T15</u>	<u>T14</u>	<u>T15</u>	<u>T14</u>	<u>T15</u>	<u>T14</u> -----	<u>T15</u>
Analysis at 2500 lb (before audible fiber damage):								
$\epsilon_x$	142	-227	325	-207	207	-182	337	-222
$\epsilon_y$	-7	201	-449	249	-554	249	-525	273
$\gamma_{xy}^a$	$\pm 64$	$\pm 3$	$\pm 118$	$\pm 96$	$\pm 49$	$\pm 139$	$\pm 72$	$\pm 99$

Analysis at 4000 lb:

$\epsilon_x$	226	-363	735	-452	386	-306	1069	-723
$\epsilon_y$	-11	322	-998	522	-993	421	-1763	958
$\gamma_{xy}^a$	$\pm 103$	$\pm 5$	$\pm 93$	$\pm 142$	$\pm 79$	$\pm 279$	$\pm 106$	$\pm 75$

a. Strain gages were not oriented consistently.

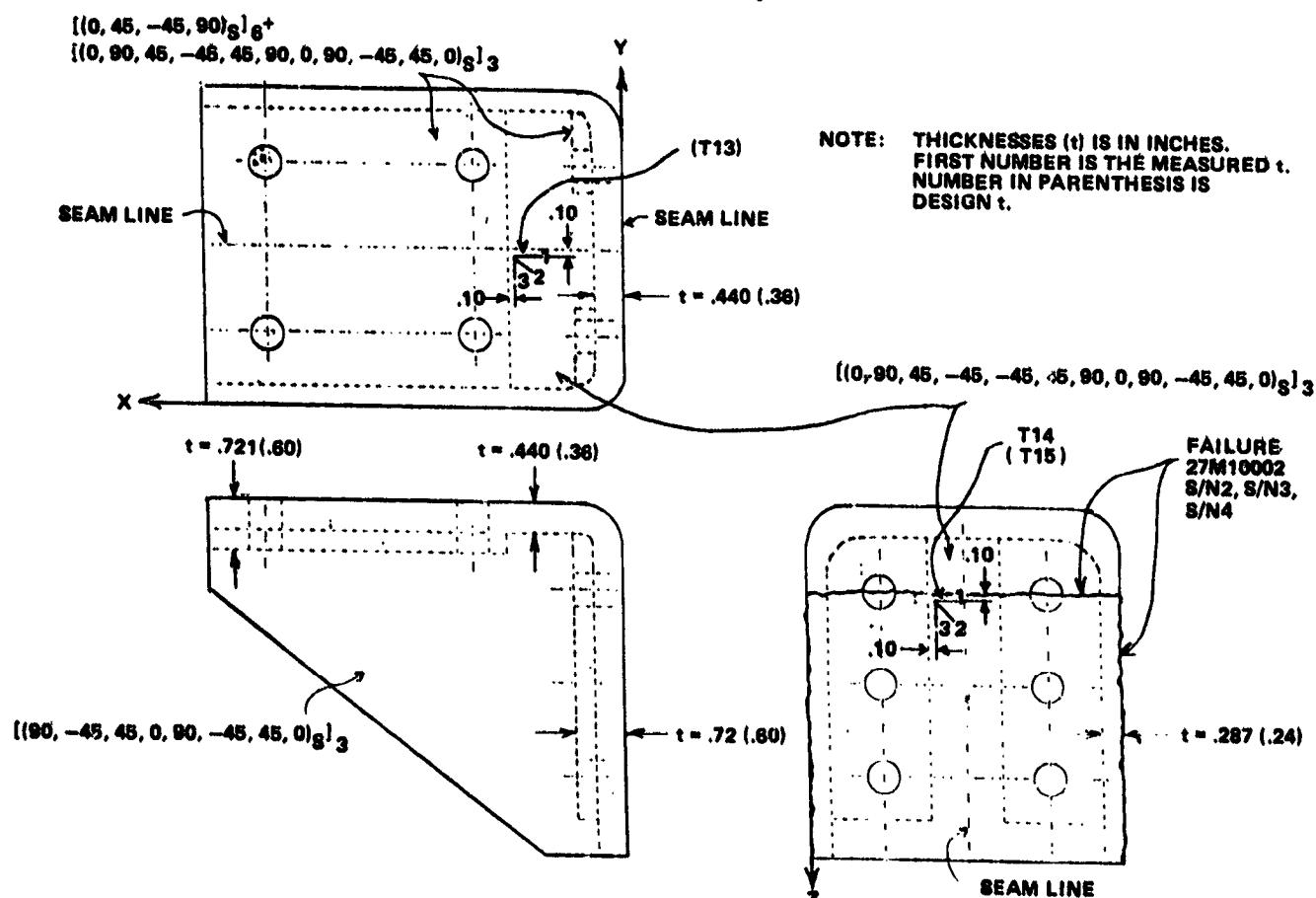


Figure 12. Strain gage and failure locations.

### 3. 27M10003 Test Results

Tables 14 through 16 present strain gage test data. Tables 17 and 18 present comparison of test and analytical results. Locations of strain gages are presented on Figure 13. S/N2 and S/N3 failed across the bolt holes on the x-face at an average load of 3463 lb. S/N1 was not retrofitted with a radius insert and failed across the bolt holes and stiffener on the z-face at a load of 2229 lb.

TABLE 14. 27M10003-STRAIN GAGE TEST DATA ( $\mu\text{in./in.}$ )

Load (lb)	1T13			2T13			3T13		
	<u>S/N1<sup>a</sup></u>	<u>S/N2</u>	<u>S/N3</u>	<u>S/N1<sup>a</sup></u>	<u>S/N2</u>	<u>S/N3</u>	<u>S/N1<sup>a</sup></u>	<u>S/N2</u>	<u>S/N3</u>
500	273	158	79	239	118	27	94	9	-6
1000	526	337	152	430	248	49	152	30	-12
1500	1015	550	246	763	400	79	137	55	-9
2000	1938	796	355	1387	585	128	-58	91	-3
2500		1057	504		806	222		134	21
3000		1340	717		993	383		176	64
3100		1410	760		1057	434		188	82
3200		1571	811		1157	483		179	88
3500			963			635			125
3600			1030			757			131

a. Did not have radius insert

TABLE 15. 27M10003 STRAIN GAGE TEST DATA ( $\mu\text{in./in.}$ )

Load (lb)	1T14			2T14			3T14		
	<u>S/N1<sup>a</sup></u>	<u>S/N2</u>	<u>S/N3</u>	<u>S/N1<sup>a</sup></u>	<u>S/N2</u>	<u>S/N3</u>	<u>S/N1<sup>a</sup></u>	<u>S/N2</u>	<u>S/N3</u>
500	82	55	46	-12	-43	-40	-116	-125	-113
1000	164	109	91	-30	-97	-88	-238	-268	-235
1500	270	167	137	-55	-152	-143	-375	-414	-369
2000	389	231	188	-112	-209	-201	-536	-576	-512
2500		307	243		-255	-256		-737	-664
3000		465	316		-291	-304		-1045	-832
3100		525	337		-328	-310		-1185	-871
3200		598	352		-358	-316		-1401	-908
3500			416			-344			-1026
3600			459			-411			-1167

a. Did not have radius insert.

TABLE 16. ...27M10003 STRAIN GAGE TEST DATA ( $\mu\text{in./in.}$ )

Load (lb)	1T15			2T15			3T15		
	<u>S/N1<sup>a</sup></u>	<u>S/N2</u>	<u>S/N3</u>	<u>S/N1<sup>a</sup></u>	<u>S/N2</u>	<u>S/N3</u>	<u>S/N1<sup>a</sup></u>	<u>S/N2</u>	<u>S/N3</u>
500	-52	-46	-58	0	6	3	76	70	67
1000	-106	-97	-118	9	12	9	155	140	133
1500	-179	-149	-185	21	27	18	237	215	212
2000	-243	-203	-246	55	40	30	309	297	297
2500		-258	-304		36	46		382	391
3000		-367	-370		6	61		531	503
3100		-392	-383		30	61		588	525
3200		-410	-398		52	61		676	546
3500			-437			67			619
3600			-577			161			940

a. Did not have radius insert.

TABLE 17. 27M10003 COMPARISON OF TEST AND SQ5 RESULTS ( $\mu\text{in./in.}$ )

	<u>SQ5 T13</u>	<u>S/N1<sup>a</sup> T13</u>	<u>S/N2 T13</u>	<u>S/N3 T13</u>
$\epsilon_x$	-353 <sup>c</sup>	526	337	152
$\epsilon_y$	-46	152	30	-12
$\gamma_{xy}$ <sup>b</sup>	$\pm 12$	$\pm 182$	$\pm 129$	$\pm 42$

a. Did not have radius insert.

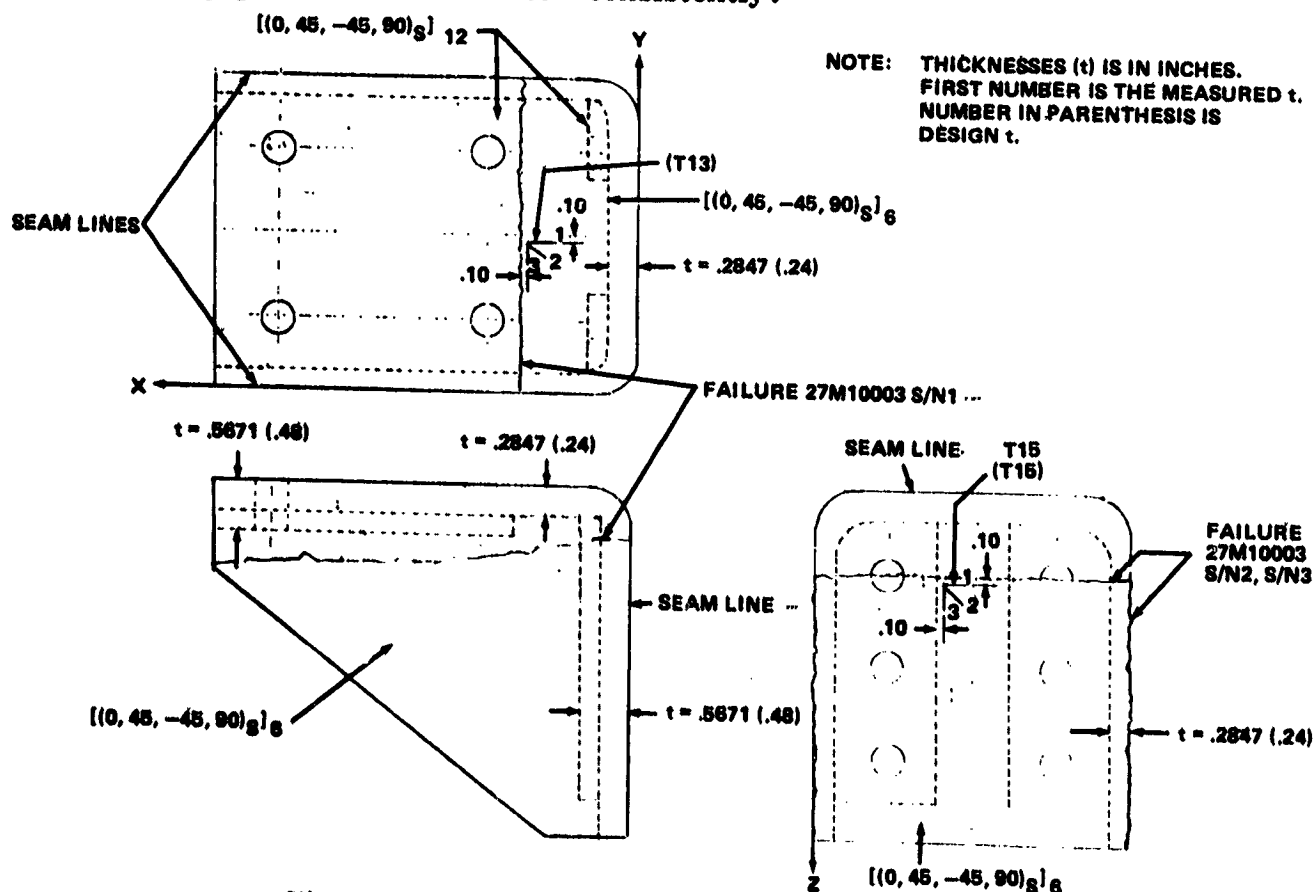
b. Strain gages were not oriented consistently.

c. Probable test polarity problem. This surface is in compression.

TABLE 18. 27M10003. COMPARISON OF TEST AND SQ5 RESULTS ( $\mu\text{in./in.}$ )

	SQ5		S/N1 <sup>a</sup>		S/N2		S/N3	
	T14	T15	T14	T15	T14	T15	T14	T15
Analysis at 1000 lb (before audible fiber breakage):								
$\epsilon_x$	72	-121	164	-106	109	-97	91	-118
$\epsilon_y$	-36	106	-238	155	-268	140	-235	133
$\gamma_{xy}^b$	$\pm 34$	$\pm 11$	$\pm 14$	$\pm 31$	$\pm 35$	$\pm 19$	$\pm 32$	$\pm 3$
Analysis at 2500 lb:								
$\epsilon_x$	179	-304			307	-258	243	-304
$\epsilon_y$	-91	265			-737	382	-664	392
$\gamma_{xy}^b$	$\pm 84$	$\pm 28$			$\pm 80$	$\pm 52$	$\pm 91$	$\pm 4$

- a. Did not have radius insert.  
b. Strain gages were not oriented consistently.





#### 4. 27M10009 Test Results

Tables 19 through 21 present strain gage test data. Tables 22 and 23 present comparison of test and analytical results. Locations of strain gages are presented on Figure 14. The fittings were made by bonding three laminated pieces together with Hysol EA-934. The two fittings failed along the bond lines at an average load of 3126 lb. Hysol EA-934 has an ultimate shear strength of 3100 psi. However, based on the bonding area of the sides (y-face) alone, the bond failed at 143 psi.

TABLE 19. 27M10009 STRAIN GAGE TEST DATA ( $\mu\text{in./in.}$ )

<u>Load (lb)</u>	1T13		2T13		3T13	
	<u>S/N1</u>	<u>S/N2</u>	<u>S/N1</u>	<u>S/N2</u>	<u>S/N1</u>	<u>S/N2</u>
500	94	33	106	15	47	15
1000	204	119	228	61	106	46
1500	334	267	368	158	191	115
2000	456	428	513	273	295	213
2500	556	529	647	346	401	322
3000	842	817	936	535	783	519
3100		939		611		586
3200		1109		720		686

TABLE 20. 27M10009 STRAIN GAGE TEST DATA ( $\mu\text{in./in.}$ )

<u>Load (lb)</u>	1T14		2T14		3T14	
	<u>S/N1</u>	<u>S/N2</u>	<u>S/N1</u>	<u>S/N2</u>	<u>S/N1</u>	<u>S/N2</u>
500	43	36	9	9	-46	-34
1000	85	73	21	18	-94	-67
1500	137	118	30	30	-146	-110
2000	182	167	37	34	-107	-165
2500	231	213	21	-91	-289	-423
3000	143	131	-280	-335	-664	-691
3100		134		-374		-755
3200		140		-475		-899

TABLE 21. 27M10009 STRAIN GAGE TEST DATA ( $\mu\text{in./in.}$ )

<u>Loads (lb)</u>	<u>1T15</u>		<u>2T15</u>		<u>3T15</u>	
	<u>S/N1</u>	<u>S/N2</u>	<u>S/N1</u>	<u>S/N2</u>	<u>S/N1</u>	<u>S/N2</u>
500	-30	-24	-6	0	34	27
1000	-64	-55	-12	3	67	49
1500	-100	-85	-21	-12	103	70
2000	-140	-118	-27	-18	143	97
2500	-182	-161	-24	-55	192	125
3000	-240	-197	210	67	612	313
3100		-213		55		341
3200		-252		46		414

TABLE 22. 27M10009 COMPARISON OF TEST AND SQ5 RESULTS ( $\mu\text{in./in.}$ )

Analysis at 1500 lb. (before audible fiber breakage):

	<u>SQ5 T13</u>	<u>S/N1 T13</u>	<u>S/N2 T13</u>
$\epsilon_x$	-368 <sup>b</sup>	334	267
$\epsilon_y$	-138	191	115
$\gamma_{xy}$ <sup>a</sup>	$\pm 59$	$\pm 211$	$\pm 66$

- a. Strain gages were not oriented consistently.  
b. Probable test polarity problem. This surface is in compression.

TABLE 23. 27M10009 COMPARISON OF TEST AND SQ5 RESULTS ( $\mu\text{in./in.}$ )

	<u>SQ5</u>		<u>S/N1</u>		<u>S/N2</u>	
	<u>T14</u>	<u>T15</u>	<u>T14</u>	<u>T15</u>	<u>T14</u>	<u>T15</u>
$\epsilon_x$	206	-25	137	-100	118	-85
$\epsilon_y$	-138	66	-146	103	-110	70
$\gamma_{xy}$ <sup>a</sup>	$\pm 19$	$\pm 34$	$\pm 69$	$\pm 45$	$\pm 52$	$\pm 9$

- a. Strain gages were not oriented consistently.

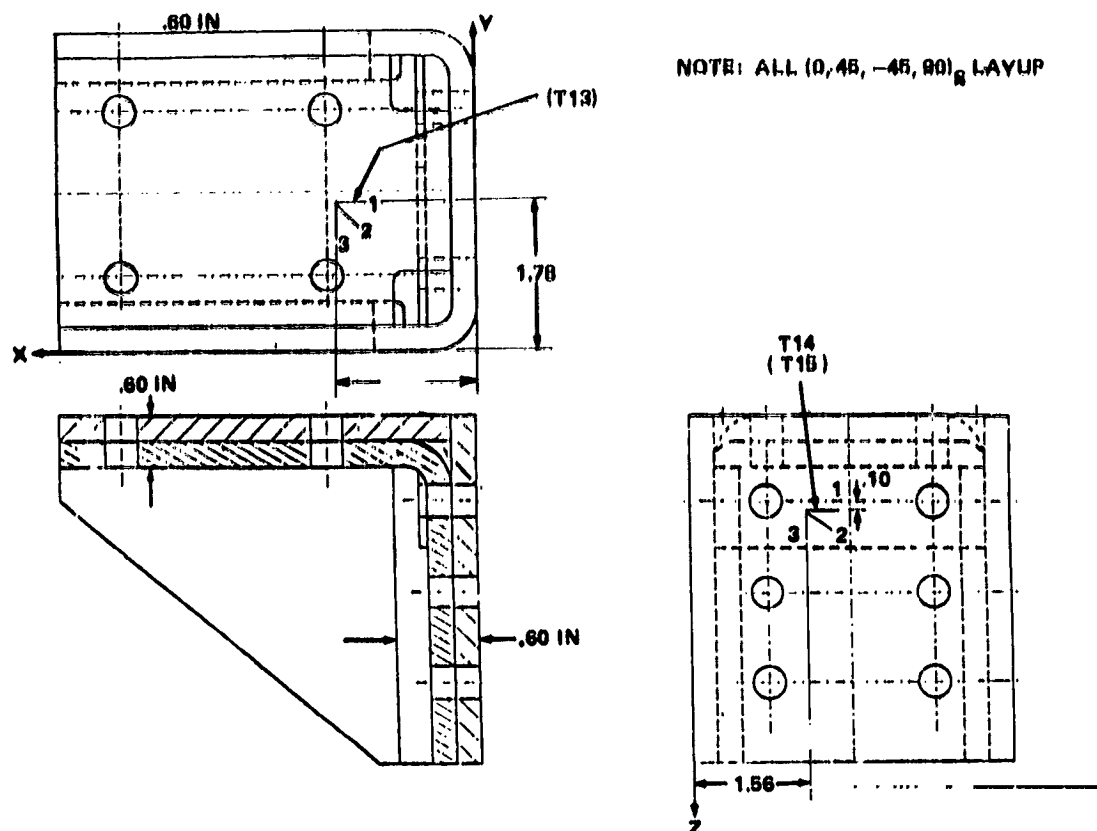


Figure 14. Strain gage locations.

## CONCLUSIONS AND RECOMMENDATIONS

27M10001, 27M10002, and 27M10003 are similar in design except for layup and seam locations. As can be concluded from the ultimate failure loads, thickness was the most important factor with 27M10002 being the thickest and strongest of the three designs. When the laminate is quasi-isotropic and balanced, thickness will determine ultimate load capability.

27M10009 failed at the lowest load even though it was the thickest of all four designs. Bonding three sections together with Hysol EA-934 was not a good design. However, this could also have resulted from faulty fabrication.

The test results did not closely correlate with the analytical results. Test results between the fittings of each configuration did not closely correlate either. The lack of correlation within a given configuration is probably due to the lack of good quality control in the fabrication process. However, this type of variation is inherent in composites.

EP42 does not have the analysis capability to redistribute loads if one or more lamina fails prior to gross failure of the laminate. Both SPAR and SQ5 perform linear analysis. The overall behavior of the laminate is nonlinear if one or more lamina fails prior to gross laminate failure. To perform adequate analysis, a 3-D finite element program that performs progressive failure analysis is required. Such a progressive failure analysis is presented in Figure 15.

ORIGINAL PAGE IS  
OF POOR QUALITY

Several problems were encountered. On the first component, the application of a kapton backing between the strain gages and the part proved very time consuming and also resulted in gage problems. The backing was eliminated for the other components. Application of gages was performed by the different groups, which negated the learning curves in applying the devices. Due to scheduling problems, the initial sequence between tests, namely a two-week spacing for data reduction and correlation, and strain gage location determination, was not maintained. Strain gage location on subsequent components were determined without the benefit of previous test results. Finally, there was the change in thickness of the fabricated parts, as mentioned before. As large variation of thickness was encountered, it made the data reduction, reanalysis and correlation between like components difficult. The same problems were present on the plate material used for material property evaluation. Even so, the obtained values appeared reasonable, accuracy could have been improved by using more time and more sample materials. A certain thickness dependence of the properties was observed in the quasi-isotropic layup, which would require additional work in the future. In general, the development program showed the need for additional experimental and analytical effort in the event of composite use for complex fittings and shapes.

Macromechanical Behavior of a Laminate - 194

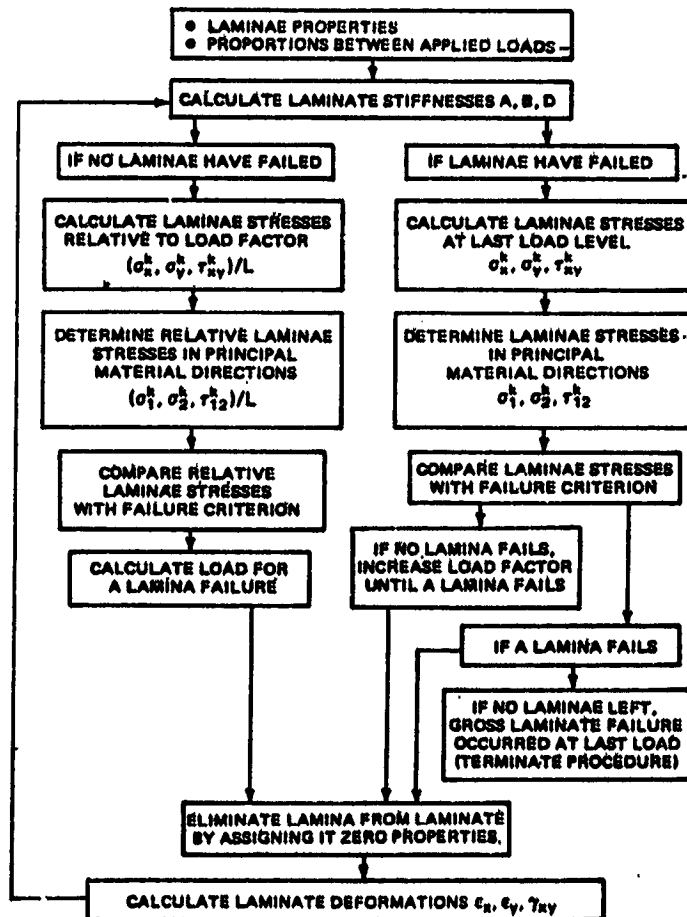


FIG. 4-24. Analysis of laminate strength and load-deformation behavior.

\* Ref: Jones, Robert M., Mechanics of Composite Materials, 1975

Figure 15. Progressive failure analysis.

APPROVAL

DEVELOPMENT AND TEST OF ADVANCED COMPOSITE COMPONENTS

By G. Faile, R. Hollis, F. Ledbetter, J. Maldonado, J. Sledd,  
J. Stuckey, G. Waggoner, and E. Engler

The information in this report has been reviewed for technical content. Review of any information concerning Department of Defense or nuclear energy activities or programs has been made by the MSFC Security Classification Officer. This report, in its entirety, has been determined to be unclassified.



C. D. Nevins, Chief  
Structures Division



P. W. Frederick, Chief  
Engineering Analysis Division



A. A. McCool, Director  
Structures and Propulsion Laboratory